



# steel research international



www.steel-research.de

## Cover Photo:

The cover image is a schematic for the utilization of hot metal up to 75% of the charge into an industrial scale 150 ton/ch DC-EAF. The steelmaking process parameters are significantly changed with the addition of large amounts of high carbon containing hot metal into the furnace. Oxygen lancing, power input, and tap-to-tap times are some of the essential process parameters that require optimization. For further details see the article by Il Sohn and co-workers on page 302.

## Publishing company:

Wiley-VCH Verlag GmbH & Co. KGaA, Boschstraße 12, D-69469 Weinheim, Germany

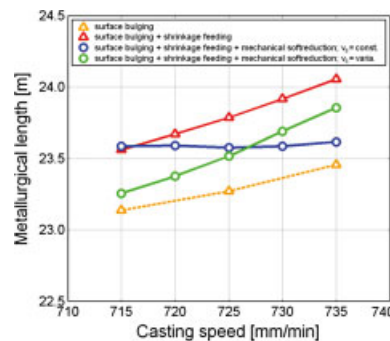
## Contents

### Technical Note

J. Domitner,\* M. Wu, and A. Ludwig

### Numerical Study About the Influence of Small Casting Speed Variations on the Metallurgical Length in Continuous Casting of Steel Slabs

184



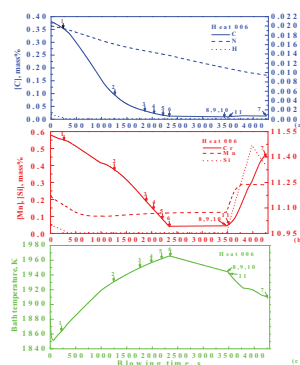
The influence of small casting speed variations ( $715\text{--}735\text{ mm min}^{-1}$ ) on the metallurgical length in steel continuous casting is numerically investigated. The numerical simulations are based on an Eulerian two-phase solidification model. For a given casting configuration, the effects of strand surface bulging, shrinkage feeding, and mechanical softreduction are considered in different simulation cases.

### Full Paper

J.-H. Wei\* and Y. Li

### Study on Mathematical Modeling of Combined Top and Bottom Blowing VOD Refining Process of Stainless Steel

189



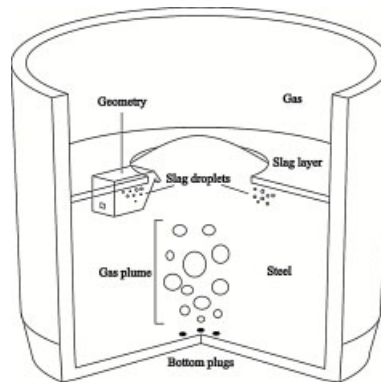
A mathematical model for the combined top and bottom blowing VOD refining of stainless steel is proposed. It is applied to 20 heats of 409L-grade steel refining in a 120 t VOD vessel, good results are obtained. The influences of the related factors and the optimization of blowing technology are examined from the model predictions.

# Contents

P. Sulasalmi,\* V.-V. Visuri, A. Kärnä, and T. Fabritius

## Simulation of the Effect of Steel Flow Velocity on Slag Droplet Distribution and Interfacial Area Between Steel and Slag

212

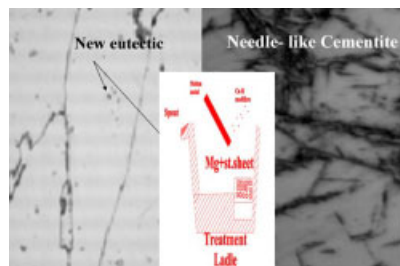


A novel approach, which combines CFD-modeling and regression analysis is applied to examine slag droplet distribution and generation rate with different steel flow velocities. Three phase CFD calculations are carried out for determining the shape of the distributions and then Rosin–Rammler–Sperling distribution function is fitted to the data, which enable estimating the birthrates of the emulsified droplets.

M. K. El Fawkhry,\* A. M. Fathy, and M. M. Eissa

## New Energy Saving Technology for Producing Hadfield Steel to High Gouging Applications

223

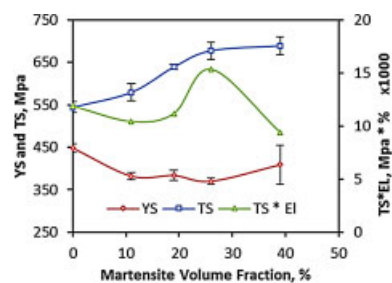


Cementite is commonly failure causing phase in steel alloys, in particular in high manganese steel. The new ladle treatment technology is used for treating molten Hadfield steel by iron base modifiers with (Mg + Ca–Si). Pseudo-eutectic is forming between austenite and cementite as a result of the ladle treatment. A new eutectic is well dispersed throughout the austenite matrix, and accordingly supplies the steel with high toughness accompanied with excellent abrasion resistance without high energy heat treatment process.

T. Allam\* and M. Abbas

## Mechanical Properties, Formability, and Corrosion Behavior of Dual Phase Weathering Steels Developed by an Inter-Critical Annealing Treatment

231



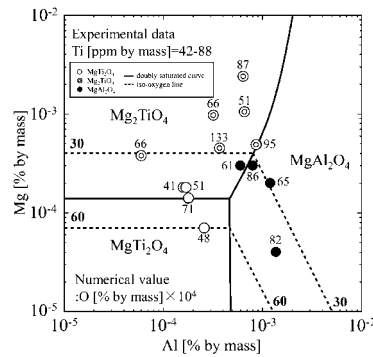
Inter-critical annealing treatments are conducted on hot-rolled weathering steel aiming at improving its mechanical and formability properties by generating DP microstructures. The developed DP-weathering steels achieve 23–25% increase in strength compared to the ferrite/pearlite weathering steel. Generating DP microstructure improve the formability to a large extent and accelerate the nucleation of the characteristic (atmospheric corrosion resistance) FeOOH layer.

# Contents

H. Ono,\* K. Nakajima, S. Agawa, T. Ibuta,  
R. Maruo, and T. Usui

## Formation Conditions of $Ti_2O_3$ , $MgTi_2O_4$ , $Mg_2TiO_4$ , and $MgAl_2O_4$ in Ti–Mg–Al Complex Deoxidation of Molten Iron

241

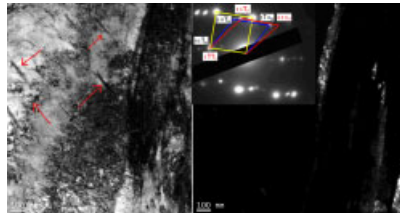


The relationships of the compounds in the Mg–Ti–Al–O system in equilibrium with molten iron are clarified at temperatures ranging from 1873 to 1973 K, and the thermodynamic calculations are conducted in avoiding  $Al_2O_3$  or spinel  $MgAl_2O_4$  formation and for inclusion control. It is shown that the equilibrium relations between those compounds and the composition of solutes in steel at 1973 K.

N. Zhong,\* Q. L. Wu, Y. S. Yin, and  
X. D. Wang

## Microstructural Evolution of a Medium Carbon Advanced High Strength Steel Heat-Treated by Quenching– Partitioning Process

252

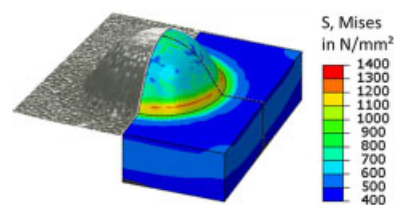


The present study shows that good combination of high tensile strength and relatively high ductility of a microalloyed carbon steel have been attained by quenching–partitioning–tempering process. The experimental results show that the sample partition-tempered for 30 s exhibits best comprehensive mechanical properties, which result from the integrated effect of carbide precipitation, conservation of certain amount of retained austenite and softening of the martensite matrix during the partition-tempering process.

A. Szurdak\* and G. Hirt

## Finite Element Analysis of Manufac- turing Micro Lubrication Pockets in High Strength Steels by Hot Micro- Coining

257

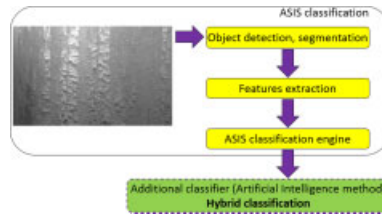


The manufacturing of micro lubrication pockets in stainless steel AISI 304 by hot micro-coining is investigated conducting finite element simulations and complementing experiments. Suitable process parameters and process limits are determined in this work. Process limits occurred for the coining of high strength materials at low process temperatures due to plastic deformation of the die.

# Contents

S. Lechwar,\* Ł. Rauch, and M. Pietrzyk  
**Use of Artificial Intelligence in Classification of Mill Scale Defects**

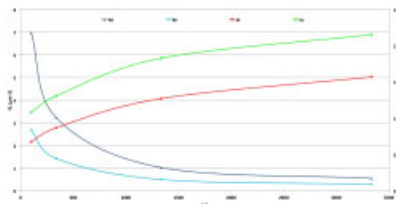
266



In this study, a classification model is developed for real-time prediction of various kinds of mill scales at typical hot rolling mill (HRM). In order to obtain input data, the automatic surface inspection system (ASIS) is used together with its classification model. Thereafter, novel procedure is introduced for further boosting of the accuracy of predictions by the use of hybrid classification concept.

E Vodopivec,\* F Kafexhiu, and B. Žužek  
**Change of  $M_{23}C_6$  Particles Size and Spacing by Tempering a High-Chromium Creep Resistant Steel at 800–550 °C**

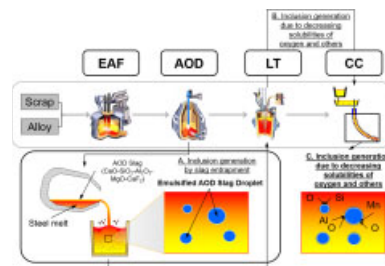
278



$M_{23}C_6$  particles size, number and dissolution velocity were deduced for tempering of a X20 steel at 800 to 550 °C. The dissolution of small particles increases the particle spacing for above one order of magnitude more than particles coarsening. By creep tests above 550 °C, particles spacing and creep rate are increased significantly by dissolution of small particles.

J.-Y. Choi, S.-K. Kim, Y.-B. Kang, and H.-G. Lee  
**Compositional Evolution of Oxide Inclusions in Austenitic Stainless Steel during Continuous Casting**

284

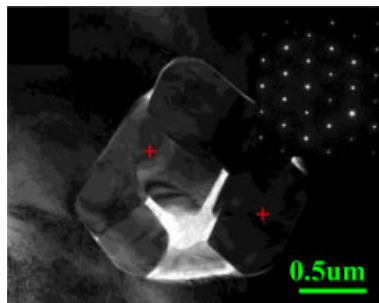


Composition evolution and number density of oxide inclusions in austenitic stainless steel during continuous casting are demonstrated by plant data as well as mathematical modeling. Origin of the inclusions is argon oxygen decarburization (AOD) slag, and the inclusions grow by subsequent oxide formation due to decrease of solubility limit of O, Al, Mn, Si, etc, during casting. A simple mathematical model is presented to account for the composition evolution.

# Contents

Q. Wu,\* W. Li, N. Zhong, and G. Wang  
**Microstructure and Properties of  
 Laser-Clad  $\text{Mo}_2\text{NiB}_2$  Cermet Coating  
 on Steel Substrate**

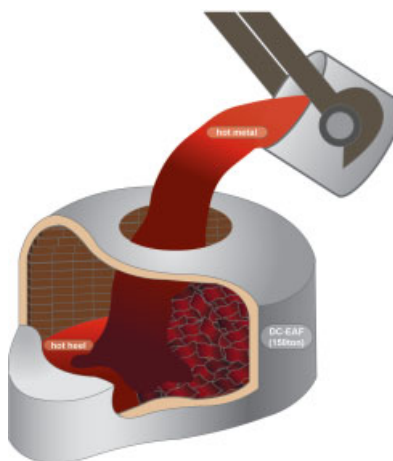
293



A novel method to synthesize  $\text{Mo}_2\text{NiB}_2$  boride cermet coating on Q235 steel substrate, consisting of  $\text{Mo}_2\text{NiB}_2$ -type ternary boride as a reinforced phase and a  $\gamma$ -(Fe, Ni) base binder, is realized with laser cladding technique. The wear resistance of the Q235 substrate is greatly improved. As compared to 304 stainless steel, lower corrosion rate is obtained for the coating and pitting corrosion disappears in particular.

B. Lee, J. W. Ryu, and I. Sohn\*  
**Effect of Hot Metal Utilization on the  
 Steelmaking Process Parameters in  
 the Electric Arc Furnace**

302



Hot metal additions into a 150 ton DC-EAF is studied. 1700 kWh of accumulated power consumption is decreased for every ton of hot metal utilized. Oxygen lancing practices is modified with hot metal additions in the EAF without increasing the tap-to-tap times. At hot metal additions of above 0.6, the decarburization rate linearly increases with oxygen lancing.